REPORT DOCUMENTATION PAGE

Form Approved
OMB NO. 0704-0188

1. AGENCY USE ONLY (Leave Blank)	2. REPORT DATE	3. REPORT TYPE AND DATES COVERED
	29 August, 2001	final report: 1 June 1998 -31 May 2001

4. TITLE AND SUBTITLE
Optical Approach to Quantum Computing

5. FUNDING NUMBERS
DAAG55-98-1-0368

6. AUTHOR(S)
James D. Franson

7. PERFORMING ORGANIZATION NAME(S) AND ADDRESS(ES)
Johns Hopkins University
Applied Physics Laboratory
11100 Johns Hopkins Rd, Laurel, MD 20723-6099

8. PERFORMING ORGANIZATION REPORT NUMBER
AROJDF3

9. SPONSORING / MONITORING AGENCY NAME(S) AND ADDRESS(ES)
U. S. Army Research Office
P.O. Box 12211
Research Triangle Park, NC 27709-2211

10. SPONSORING / MONITORING AGENCY REPORT NUMBER
38792.16-PH-QC

11. SUPPLEMENTARY NOTES
The views, opinions and/or findings contained in this report are those of the author(s) and should not be construed as an official Department of the Army position, policy or decision, unless so designated by other documentation.

12 a. DISTRIBUTION / AVAILABILITY STATEMENT
Approved for public release; distribution unlimited.

12 b. DISTRIBUTION CODE

13. ABSTRACT (Maximum 200 words)

The primary goal of this project was to investigate the possible use of photon-exchange interactions to implement quantum logic gates. The nonlinear phase shifts produced by photon-exchange interactions were investigated theoretically using several different methods, including Dicke-state expansions of the excited atoms in a medium and density-matrix calculations to include the effects of collisions and spontaneous emission. An experimental investigation was performed in which two single photons were propagated through a sodium vapor cell with a laser pulse applied at the same time. The experimental results demonstrated a small nonlinear phase shift, as expected from the theoretical calculations. Errors in which the laser pulses do not return the atoms to their initial state may limit the practical applications of this approach.

14. SUBJECT TERMS
Nonlinear Optics Low-intensity Quantum computer Quantum logic

15. NUMBER OF PAGES
18

16. PRICE CODE

17. SECURITY CLASSIFICATION OR REPORT	18. SECURITY CLASSIFICATION ON THIS PAGE	19. SECURITY CLASSIFICATION OF ABSTRACT	20. LIMITATION OF ABSTRACT
UNCLASSIFIED	UNCLASSIFIED	UNCLASSIFIED	UL

FINAL PROGRESS REPORT

Optical Approach to Quantum Computing

ARO contract # DAAG55-98-1-0368
Work supported by ARDA, ARO, and NSA

J. D. Franson, Principal Investigator
Johns Hopkins University
Applied Physics Laboratory
Laurel, MD 20723

I. Foreword

An optical approach to quantum computing would have a number of potential advantages, including the ability to connect quantum logic and memory devices using optical fibers or waveguides. Other potential advantages include high speed and a low coupling to the environment. On the other hand, any optical approach to quantum computing will require nonlinear interactions between single photons in order to perform quantum logic operations, which are inherently nonlinear. Conventional mechanisms for nonlinear optics are essentially classical in nature and generally too weak to be used for single-photon interactions. The main goal of this project was to investigate a nonclassical mechanism for producing nonlinear phase shifts based on photon-exchange interactions. The basic physics behind this approach was investigated both theoretically and experimentally. Several different theoretical analyses showed that nonlinear phase shifts could be produced using photon-exchange interactions in an atomic medium accompanied by one or more intense laser pulses that are off-resonant. An experiment in sodium vapor demonstrated nonlinear phase shifts in rough agreement with the theory. The observed nonlinear phase shifts were relatively small for technical reasons, but a nonlinear phase shift of π should be achievable by modifying the experimental conditions. It was found, however, that the nonlinear phase shifts were accompanied by relatively large errors in which the atomic system was left in the incorrect state by the laser pulse. An attempt was made to reduce the magnitude of these errors using a sequence of laser pulses and additional photons (ancilla), but substantial errors in the logic operations may be unavoidable. As a result, we are now pursuing a hybrid approach in which cooperative effects of this kind would be used for single-photon memory devices while a combination of linear optical elements and post-selection would be used for the logic operations.

II. Table of Contents

III. List of Illustrations

IV. Statement of the Problem

As discussed in the foreword, the basic goal was to investigate the use of photon-exchange interactions for the production of nonlinear phase shifts which, in turn, could be used to implement quantum logic operations. Several different kinds of theoretical analysis are described below in section A. An experimental investigation of the predicted results from the analysis is discussed in section B.

A. Theoretical analysis

The generation of a nonlinear phase shift by photon-exchange interactions can be intuitively understood from Fig. 1, which illustrates two single photons incident on a medium containing N atoms. A typical pair of atoms is labeled A and B. The photons are assumed to be far off resonance from the excited states of the atoms, in which case either atom can briefly absorb either photon in a virtual process. Since there are two different ways to produce a state in which both atoms are excited (either photon can excite either atom), the probability of such a state is enhanced by a factor of 2 due to quantum interference. Either atom can then re-emit either photon, which we refer to as an exchange process. Such a process can only occur if both photons are in the medium at the same time and it is inherently nonlinear in that sense. If a short laser pulse is applied to the medium at the same time that both atoms are excited, a Stark shift will produce a phase shift in the overall state of the system that is nonlinear, since the population of the excited states is larger by a factor of 2 when both atoms are present. This intuitive argument was verified using several different theoretical approaches, as described below.

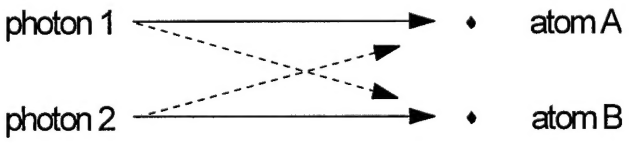

Fig. 1. Photon-exchange interaction produced when two photons are virtually absorbed and re-emitted in an atomic medium.

Our original analysis was based on the assumption that the medium is thin compared to the length of the incoming photon wave packets. In that case, all of the atoms are subjected to the same electric field from the photons and we cannot distinguish which atom is excited. This allows the system to be described by an effective state vector with only six states:

$$|\psi\rangle_{eff} \equiv \begin{pmatrix} c(\gamma_1,\gamma_2) \\ c(\gamma_1) \\ c(\gamma_2) \\ c(0) \\ c(\gamma_1,\gamma_1) \\ c(\gamma_2,\gamma_2) \end{pmatrix} \tag{1}$$

Here the various coefficients correspond to the probability amplitude that both photons are present, photon 1 has been absorbed, photon 2 has been absorbed, both photons have been absorbed, etc. We showed that this system satisfies Schrodinger's equation with an effective Hamiltonian given by

$$H'_{eff} = \begin{bmatrix} 0 & \sqrt{N}M & \sqrt{N}M & 0 & 0 & 0 \\ \sqrt{N}M & -\delta_2 & 0 & \sqrt{2(N-1)}M & \sqrt{2N}M & 0 \\ \sqrt{N}M & 0 & -\delta_1 & \sqrt{2(N-1)}M & 0 & \sqrt{2N}M \\ 0 & \sqrt{2(N-1)}M & \sqrt{2(N-1)}M & -(\delta_1+\delta_2) & 0 & 0 \\ 0 & \sqrt{2N}M & 0 & 0 & (\delta_1-\delta_2) & 0 \\ 0 & 0 & \sqrt{2N}M & 0 & 0 & (\delta_2-\delta_1) \end{bmatrix} \tag{2}$$

where the various constants will not be described here. Schrodinger's equation was solved to give the state vector as a function of time in the adiabatic limit. The results of the analysis showed that the interaction with the medium produces a two-photon dressed state which is analogous to the well-known single-photon dressed states. The calculations also verified the factor of 2 due to quantum interference and the production of a nonlinear phase shift when a laser pulse is applied to the medium.

A thick medium is required to produce a nonlinear phase shift of π for quantum logic operations. In that case, however, the atoms are subjected to different electric fields with different phase factors. We were able to generalize our analysis to the case of a thick medium by expanding the excited states of the atoms in the medium using Dicke states, which can be generated using operators that are analogous to angular momentum raising and lowering operators:

$$\hat{R}_{\pm}(\boldsymbol{p}) = \hat{R}_1(\boldsymbol{p}) \pm i\hat{R}_2(\boldsymbol{p}) = \sum_j \hat{R}_{\pm}^{(j)} e^{\pm i\boldsymbol{p}\cdot\boldsymbol{r}_j}. \quad (3)$$

These operators create a superposition of excited atoms with a plane-wave phase dependence. Because of conservation of momentum (k-vectors), the absorption of a photon produces a single Dicke state. As a result, the system reduces to a six-state effective state vector similar to that described above. The results of this analysis also showed the factor of 2 enhancement and the production of nonlinear phase shifts that were obtained from the simpler case of a thin medium. In addition, the Dicke-state analysis showed that the N^2 dependence of the nonlinear phase shift follows directly from the cooperative nature of the Dicke-state excitations. It was also shown that the scattering of the photons can be neglected for a thick, uniform medium.

The analysis was generalized further to include the effects of collisions and spontaneous emission, which are important sources of decoherence in an atomic medium. Dissipative effects of this kind can only be included in a density-matrix calculation. Numerical delnsity-matrix calculations were performed using the quantum trajectories approach and the Dicke-state expansion described above. The results of this analysis show most of the features observed in the experiments, as will be discussed below, but more detailed calculations are still in progress in order to improve the agreement with the experimental results before they are published.

Our theoretical analyses showed that a single laser pulse will produce a nonlinear phase shift but will also leave the system in the incorrect final atomic state some fraction of the time. We made a considerable effort to design a sequence of laser pulses that would produce a nonlinear phase shift of π while returning the system exactly to the same final state. We also included up to four additional photons (ancilla) in an effort to reduce the probability that the system will be left in the wrong final state. Although sequences of laser pulses and ancillas can reduce the overall error, we were unable to completely eliminate all errors of this kind, which may be a limiting factor in practical applications of this approach.

B. Experimental investigations.

The goal of the experimental investigations was to verify the basic physical interactions described above. In order to simplify the initial experiments, we used a thin medium with large detunings and a single laser pulse. As a result, the expected nonlinear phase shift was relatively small ($\sim 1°$), since most of the photon wave packet was not inside the atomic medium at the time the laser pulse was applied.

The experiment consisted of propagating two single-photon wave packets through a sodium vapor cell, either at the same time or at times differing by 13 ns. A short laser pulse was applied coincident with the photon wave packets (every 13 ns), which was expected to produce a nonlinear phase shift if both photons were present. The polarizations of the photons were chosen in such a way that the presence of photon 1 (control) should rotate the polarization of photon 2 (target) by a small

amount due to a nonlinear birefringence. This effect could be detected using a polarization analyzer and coincidence electronics. The results were then compared for the cases in which the photons passed through the medium at the same or two different times.

A schematic diagram of the experiment is shown in Fig. 2 and a photograph of the apparatus is shown in Fig. 3. The two single-photon wave packets originate from a Coherent Model 899 tunable dye laser. The dye laser uses Rhodamine 6G as a gain medium, and is operated in a uni-directional ring cavity configuration that produces a continuous-wave (cw) output beam whose linewidth is roughly 20 MHz. The dye laser is pumped by a Coherent Innova 300 Argon-Ion laser whose output is roughly 3 to 4 Watts at 514 nm. The final output power of the dye laser is typically on the order of 50 mW. Birefringent polarization tuning elements inside the ring cavity allow the dye laser to be scanned over a very broad wavelength range (roughly 100nm), and set on a coarse scale to the desired operating wavelength of 589 nm, which corresponds to the ground state D_1 transition of sodium. Fine-tuning of the operating frequency is done by a computer controlled scanning Brewster plate inside the ring cavity that allows continuous tuning over a range of 30 GHz. The frequency of the laser is accurately calibrated by sending part of the output beam through a sodium reference lamp and performing absorption spectroscopy. This ultimately allows us to accurately set the detunings of the single photons from the resonance.

The cw laser beam at the desired detuning is then sent through an amplitude modulator, which is used to generate short duration optical pulses. The amplitude modulator consists of a custom made ConOptics Model 1000 Laser Modulation System. It utilizes ultra fast electronics and the optical Pockels effect to produce a fast and temporary rotation of the polarization of the input beam, which can then pass through an orthogonally oriented Glan-Thompson polarizer. The ConOptics Pockels cell unit is driven by an amplified 76 MHz rf signal that is synchronized with an additional mode-locked pulsed laser as will be described below. The duration of the optical output pulses is ultimately what determines the temporal width of the single photon wave packets, and is therefore a critical parameter of the experiment. The state-of-the-art ConOptics unit is able to produce optical pulses that are roughly 3ns FWHM. In summary, the cw input to the amplitude modulator is chopped into an output train of pulses that are each 3ns wide, and separated by 13.2ns (eg., 1 over 76 MHz).

These pulses then pass through a New Focus, Inc. Model 4431 bulk phase modulator. When driven by a sinusoidal rf input signal, this phase modulator is able to generate frequency sidebands on the central carrier frequency, ω_0. These sidebands appear at the central carrier frequency plus or minus all integral multiples of the driving frequency. The amplitude of the various sidebands have a Bessel function dependence on the rf power. The New Focus unit is driven by a Hewlett-Packard function generator set to produce a 2.5 GHz Sine wave. We typically operate the phase modulator in the strongly driven regime, where the magnitude of the first-order sidebands at $\omega_1 = \omega_0 - 2.5$ GHz and $\omega_2 = \omega_0 + 2.5$ GHz are comparable to the remaining amplitude at ω_0.

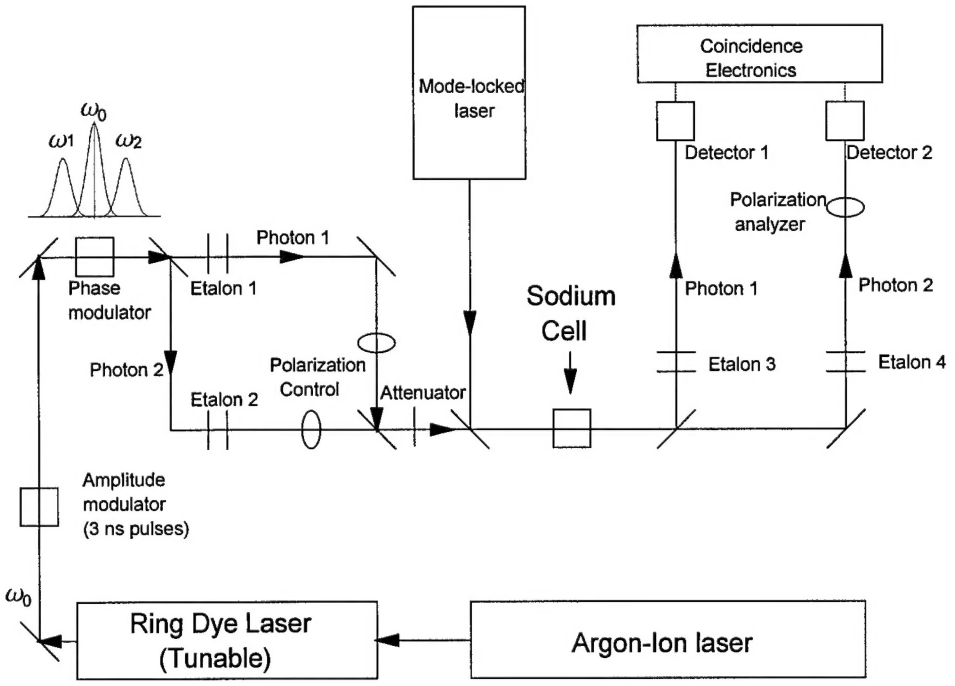

Fig. 2. Outline of the experimental apparatus.

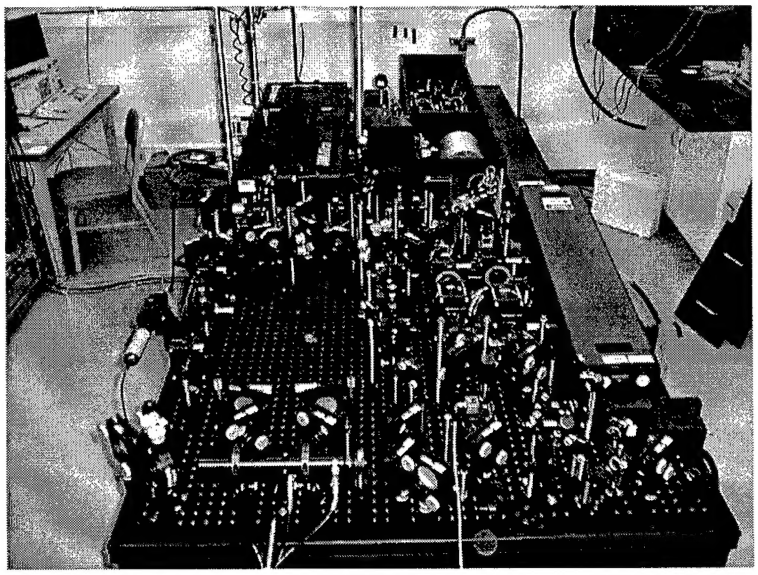

Fig. 3. Photograph of the experimental apparatus.

After passing through the phase modulator, each of the optical pulses can be thought of as containing many photons at the original carrier frequency ω_0, as well as many photons at each of the sideband frequencies ω_1 and ω_2. It is these frequency sidebands at ω_1 and ω_2 that will ultimately serve as the two single photons, photon 1 and photon 2. The optical beam containing these pulses is then split with a 50/50 beamsplitter which has a Fabry-Perot etalon in each of its output port optical paths. The etalons are air-spaced with a 10 mm gap, and have a free spectral range of 15 GHz and a finesse of about 30. Prior to entering the etalons, each of the beams is expanded and collimated to reduce divergence and minimize the effective frequency bandpass of the etalons. In our system the minimum achievable bandpass was measured to be roughly 1 GHz FWHM. This allows each of the etalons to pass one of the three possible frequencies (ω_0, ω_1, or ω_2), while rejecting the other two frequencies. Each of the etalons is tilt-tuned on the arc second level using computer-controlled motorized micrometers. Etalon 1 serves as the master etalon, and has its peak transmission locked at a fixed frequency detuning relative to the sodium reference lamp. Etalon 2 is then tuned and locked (relative to etalon1) to pass only photons of frequency $\omega_2 = \omega_1 +$ 5 GHz. Typical detunings for the experiment are δ_1=6 GHz and δ_2=11 GHz.

Following the beam splitter, photons of frequency ω_1 travel along the lower path while photons of frequency ω_2 travel along the upper path. A combination of waveplates is placed in each of these paths and allows complete control of the polarization of each of the beams. As will be discussed in the next section, photons at ω_1 serve as the "control" photons and are linearly polarized in the vertical direction. Photons at ω_2 serve as the "target" photons and are linearly polarized at 45 degrees with respect to the vertical axis.

The two beams are then recombined using another 50/50 beamsplitter. To ensure that the two beams are merged into the same mode, the common output beam of the beam splitter passes through a spatial filter consisting of two achromatic lenses surrounding a 10 micron diameter pinhole. Each of the beams (photon 1 and photon 2) is aligned for maximum transmission through the spatial filter using sub-micron resolution computer-controlled motorized mirror mounts manufactured by Burleigh, Inc.

The output of the spatial filter is therefore effectively a single beam containing a train of 3ns wide optical pulses at frequency ω_1 (with vertical polarization) overlapping a coincident train of 3ns wide optical pulses at frequency ω_2 (with 45 degree polarization). Using neutral density filters, this beam is attenuated down to level where the probability of having even a single photon in either of the pulses is much less than one. The probability of detecting two photons is proportional to α^2, where $\alpha << 1$ corresponds to the probability of having a single photon 1 or photon 2 wave packet contained in a given optical pulse. Higher order correlations involving more than two photons are proportional to terms of order α^3 or smaller and can be safely neglected. As a result, those pulses that are found by a post-selection process to contain a single photon at ω_1 are equivalent to having used a true single-photon source for those events.

As described earlier, additional high-intensity laser pulses are used to perturb the excited states of the sodium atoms in the vapor cell. These laser pulses are derived from a Coherent Mira mode-locked Ti-Sapphire laser, as shown in Figure 2. The Ti-Sapphire rod of the Mira is pumped by 5 Watts of 532 nm radiation from a Coherent Verdi solid-state laser system. The Verdi is essentially a frequency-doubled Nd:Yag laser that is designed for the long-term power stability that is required for mode-locking of the Mira.

The Mira achieves passive mode-locking by a Kerr-lens self-focusing effect and utilizes an internal Gires-Tournois Interferometer (GTI) as a cavity end mirror for group velocity dispersion compensation. The GTI and cavity are optimized to provide 8 picosecond output pulses at a repetition rate of 76 MHz. The average output power of the Mira is just below 1 Watt (e.g. several nanojoules per pulse). Special optical element coatings and birefringent tuning elements inside the Mira cavity allow the central frequency of the pulses to be continuously tuned over a wavelength range of about 50 nm. In our experiment, the operating frequency is typically tuned to be roughly 50 GHz from the 819 nm excited state transition.

The output of the Mira passes through a Faraday isolator to eliminate any backscattering that could break the sensitive mode-locked operation. The beam then passes through a rotatable waveplate followed by a vertical polarizer. This preserves the vertical polarization of the Mira while allowing the power of the beam being sent into the sodium vapor cell to be continuously increased from zero up to the full output power of the Mira.

The Mira pulses then pass through a spatial filter and are merged into the beam containing the single-photon wave packets, photon 1 and photon 2, using a dichroic beam splitter. All three beams are focused into the sodium vapor cell using an achromatic lens. The photon 1 and photon 2 beams are focused to a spot size of 50 microns in the center of the vapor cell, while the spatial filter in the Mira beam is configured in such a way that the Mira beam is focused to a spot size of 75 microns. The Rayleigh-range of all three beams is comparable to the length of the cell (1.4 cm).

Precise steering of the tightly focused Mira beam onto the photon 1 and photon 2 beams is accomplished by holding the dichroic beamsplitter in a computer-controlled motorized-micrometer-driven mount. A set of knife-edges is scanned (by another motorized micrometer) through the beam profiles to ensure proper overlap. As will be discussed later, ultra-fine scale alignment of the Mira beam is achieved by optimizing a nonlinear optical signal that originates in the atomic medium.

In order to synchronize the timing of the Mira pulses with the photon 1 and photon wave packets, a fraction of the Mira's original output beam is sent to a fast photodetector. The output of this photodetector is therefore a 76 MHz rf signal which is amplified and used to drive the amplitude modulator which creates the 3ns wide photon 1 and photon 2 wave packets. By carefully adjusting the electronic delay line which connects the photodetector to the amplitude modulator, the peaks of the Mira pulses and the single photon wave packets can be arranged to enter the vapor cell simultaneously.

The current version of the sodium vapor cell is constructed from a custom made stainless-steel chamber with sapphire windows. Earlier versions made from pyrex cells were unable to withstand the high temperatures needed to produce the desired sodium vapor pressures. It was found that as the cell temperature approached 200 °C there was a rapid migration of the sodium atoms into the pyrex walls and a corresponding degradation in the effective vapor pressure. Whereas the older pyrex cells would be degraded on a time scale ranging from several hours to several days, the new stainless-steel/sapphire cells have shown no signs of degradation after many months of operation. One additional complication of the new cell design is temperature and stress induced birefringences in the sapphire windows that do not occur in the non-crystalline pyrex. These birefringence changes can cause unwanted polarization changes on the optical beams and are compensated by adding additional waveplates before and after the cell.

The stainless-steel/sapphire cell is housed inside a custom-made oven that allows the operating temperature to be chosen anywhere in the range from room temperature up to roughly 300 °C. The oven is able to indefinitely maintain the chosen temperature to within roughly 0.5 °C.

Upon emerging from the cell, the three collinearly-propagating beams encounter another dichroic beam splitter. This beam splitter reflects the Mira pulses into a beam dump, and transmits the photon 1 and photon 2 wave packets. Additional colored Schott-glass filters and 10 nm wide interference filters centered at 589 nm are also used to eliminate any residual Mira transmission through the dichroic beamsplitter, while transmitting the photon 1 and 2 wave packets with high probability.

The common photon 1 and photon 2 beams are then re-expanded and collimated by another optical telescope. The expanded beams enter another 50/50 beam splitter which has Fabry-Perot etalons in each of its output ports. Etalon 3 and etalon 4 are temperature stabilized and have computer-controlled tilt-tuning identical to that of etalons 1 and 2. Etalon 3 has its maximum transmission locked to the master etalon 1. In this way, it transmits only photon 1 wave packets and rejects photon 2 wave packets. Conversely, etalon 4 is locked to etalon 2 and transmits only photon 2 wave packets.

The photon 1 and 2 beams are each focused onto the 1 mm^2 active area of two single-photon detectors labeled detector 1 and detector 2. In front of detector 2 is a rotatable polarization analyzer that will be described in the next section. The detectors are EG&G Inc. (recently acquired by Perkin Elmer) single photon counting modules. They are silicon avalanche photodiodes that are biased slightly above their breakdown voltages and operate in Geiger-mode with a quantum efficiency of roughly 70 %. The back half the experiment is enclosed in a dark-box which helps eliminate background detector counts from stray room lighting, equipment displays, etc.

The output pulses of each detector are sent into a Tennelec Inc. Model TC434 quad constant fraction discriminator (CFD) for pulse discrimination and reshaping. The CFD output pulses corresponding to each detector are split so that part of the signal can be used to monitor the single-detector counting rates. The other parts of the signals are sent into a coincidence counting circuit

which consists of an EG&G Ortec Model 457 time-to-amplitude converter (TAC) followed by an EG&G Ortec Model 800 analog-to-digital converter (ADC). The pulses from detector 1 are used as the start for the TAC and the pulses from detector 2 are electronically delayed and then used as the stop for the TAC. The output of the TAC is therefore an analog pulse whose height is directly proportional to the start-stop time difference. This analog pulse height is digitally binned by the ADC and sent to a multi-channel analyzer/ personal computer which plots a histogram of the number of coincidence counts registered in each of the bins as a function of the difference in the arrival times of photons 1 and 2.

The coincidence window is divided into 100 bins and is typically configured to span a delay ranging from −33 ns to +33 ns (eg. a 66 ns width). A positive delay indicates that photon 2 arrived at detector 2 after photon 1 had arrived at detector 1. Of particular interest is zero time delay, which corresponds to the case when photon 1 and photon 2 arrived at their respective detectors at exactly the same time. This implies that the two photons propagated through the sodium vapor cell at the same time, in contrast to positive or negative delays which imply that the photons propagated through the cell at different times.

A typical histogram of accumulated photon 1 – photon 2 coincidence detections is shown in Figure 4. Note that the coincidence histogram shows five distinct peaks. The peaks are separated by 13.2 ns, which directly corresponds to the repetition rate (76 MHz) of the amplitude modulator used to create the photon 1 and photon 2 wave packets. The central peak (at zero delay) corresponds to the case where photon 1 and photon 2 traveled through the vapor cell together and were detected at the same time. The peak centered at +13.2 ns corresponds to the case where photon 1 was contained in one optical pulse of the pulse train while photon 2 was contained in the following optical pulse of the train. The peak at −13.2 ns corresponds to the opposite case, and the peaks at +/- 26.4 ns correspond to the cases in which the two single photons were separated by two periods of the pulse trains. The background coincidence rate has been subtracted from these data to enhance the visibility of the differences in the peaks.

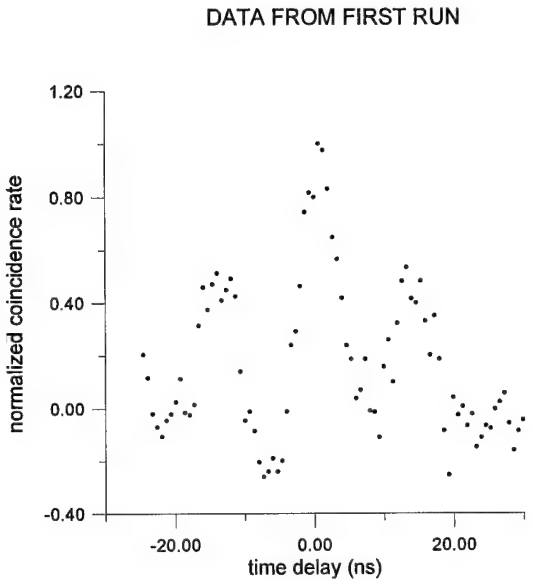

Fig. 4. Normalized coincidence rate (with background subtracted) as a function of the difference in arrival time of the two photons. The peak in at zero time delay is consistent with a nonlinear photon-photon interaction.

It can be seen that center peak is significantly larger than the other peaks, which is consistent with a photon-photon interaction as predicted by the theory. The two peaks at $\pm$ 13 ns also show a smaller enhancement, which is due to the finite lifetime of the atomic states. These results are reproducible on a day-to-day basis, but it was found that the sign of the effect oscillates rapidly as a function of the sodium density. This effect complicates our plans to measure the magnitude of the nonlinear phase shift as a function of density for comparison with the N^2 dependence predicted theoretically. The oscillations are due to the large changes in the index of refraction of the medium at the high densities and small detunings used in the experiment. A more detailed theoretical analysis that includes these factors does give oscillating central peaks but requires further work in order to give better agreement with the theory and the experiment. It is expected that the results of the experiment will be published following these enhancements to the theoretical calculations.

V. Summary of Results

More detailed calculations were performed to include realistic effects, such as collisions and spontaneous emission. These calculations confirmed the intuitive idea that photon-exchange interactions can produce a nonlinear phase shift when two photons are present in a medium subjected to a short laser pulse. They also confirmed that the effect should depend on the square of the number of atoms in the medium, which is due to the cooperative nature of the phenomena.

Experiments performed in sodium vapor cells showed that photon-exchange interactions can produce small nonlinear phase shifts as expected. The magnitude of the nonlinear phase shift was limited in these experiments by the fact that the photon wave packets were much longer than the medium. It is expected that nonlinear phase shifts on the order of π could be obtained using shorter wave packets and a longer medium. The publication of the experimental results is expected following further refinements to the theoretical model to include refractive effects in the medium.

The theoretical predictions also showed that there is a significant probability that a laser pulse will leave the atoms in a different atomic state than they occupied initially. This would correspond to a source of error in quantum-computing applications. Although we made a major effort to eliminate errors of this kind using sequences of laser pulses and ancilla photons, we were not able to completely eliminate these errors. As a result, we are currently pursuing a hybrid approach in which cooperative effects of the kind described above would be used as a single-photon memory device, while the logic operations would be performed using linear optical elements and post-selection. In particular, Knill, Laflamme, and Milburn have shown that linear optical elements, ancilla photons, and post-selection can be used to implement probabilistic logic operations that succeed with a probability typically on the order of 1/16 to 1/4. They also showed that the probability of success can be increased to nearly unity by cascading devices of this kind, which should allow a scalable approach to quantum computing.

We have recently shown that probabilistic quantum logic gates can be implemented using polarizing beam splitters and post-selection. For example, our implementation of a controlled-NOT gate is shown in Figure 5. Our approach has a number of practical advantages, including a greatly reduced sensitivity to phase drifts and a reduction in the number of detectors required. We are currently pursuing an expermental investigation of this approach using internal IR&D funding.

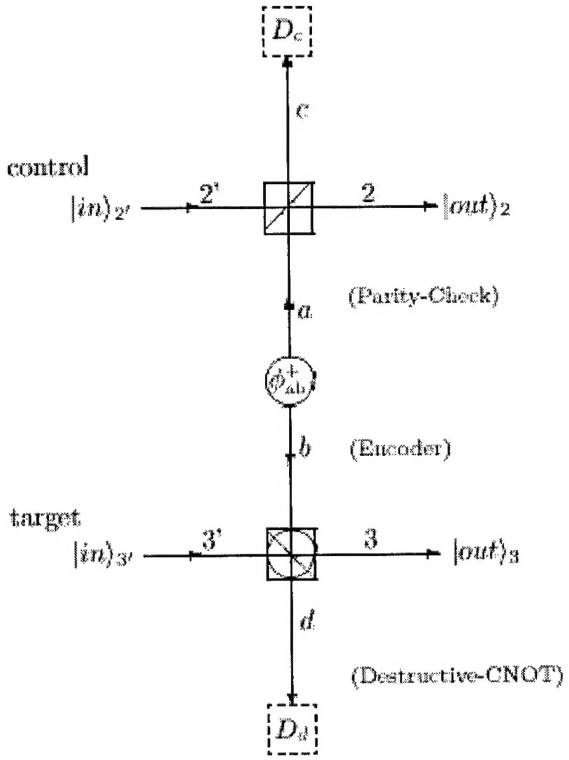

Fig. 5. Probabilistic controlled-NOT gate implemented using two polarizing beam splitters, two ancilla, and two polarization-sensitive detectors.

VI. Publications and presentations

Refereed journals and books:

J. D. Franson and T. B. Pittman, "Quantum logic operations based on photon exchange interactions", Phys. Rev. A **60**, 917 (1999).

J. D. Franson, "Reply to a Review of Photon-Exchange Interactions by Opatrny and Kurizki", Fortschritte der Physik, **48**, 1133 (2000).

J. D. Franson and T. B. Pittman, "An Optical Approach to Quantum Computing", in *Lecture Notes in Computer Science* **1509**, C. Williams, Ed. (Springer, New York, 1999).

J. D. Franson and T. B. Pittman, "Nonlocality in Quantum Computing", Fortschr. Phys. **46**, 697 (1999).

Conference presentations:

J. D. Franson, "Quantum logic using photon-exchange interactions: Theory and experiment", invited paper presented at the 31st Winter Colloquium on the Physics of Quantum Electronics, Snowbird, Utah, Jan. 7-11, 2001.

J. D. Franson, "Quantum Communications", invited tutorial presented at the Quantum Electronics and Laser Science Conference, Baltimore, MD, May 6-11, 2001.

J. D. Franson, "Quantum Communications", invited tutorial presented at the International Conference on Quantum Information, Rochester, NY, June 10-13, 2001.

J. D. Franson and T. B. Pittman, "Single-photon logic and memory, invited paper presented at the Workshop on Quantum Optics, Jackson, Wyoming, July 30-Aug 4, 2000.

J. D. Franson, "Quantum Cryptography Systems", invited paper at the IEEE 2000 Sarnoff Symposium, The College of New Jersey, March 22, 2000.

J. D. Franson," Dicke-state analysis of nonlinear phase shifts from photon-exchange interactions", invited paper presented at the Quantum Communication, Measurement, and Computing conference, Capri, Italy, July 3-7, 2000.

T. B. Pittman and J. D. Franson, "Quantum logic using photon exchange interactions", proceedings of the Quantum Electronics and Laser Science Conference, San Francisco, California, May 7-12, 2000.

J. D. Franson, "Nonlinear optics at single-photon intensities", invited paper at the 30th Winter Colloquium on the Physics of Quantum Electronics, Snowbird, Utah, January 9-12, 2000.

J. D. Franson and T. B. Pittman, "Quantum Logic Using Photon Exchange Interactions", paper presented at the OSA Annual Meeting, Santa Clara, California, Sept. 26-30, 1999.

J. D. Franson, "Photon Exchange Interactions for Quantum Logic Gates", invited paper at the TAMU/ONR Summer Workshop in Quantum Optics, Jackson Hole, WY, July 26-30, 1999.

J.. D. Franson, "Quantum logic and control using photon exchange interactions", invited paper presented at the Adriatico Research Conference on Quantum Interferometry, Trieste, Italy, 4 March, 1999.

T. B. Pittman and J. D. Franson, "Quantum logic gates using photon exchange interactions", proceedings of the Quantum Electronics and Laser Science Conference, Baltimore, MD May 24, 1999.

J.D. Franson, "Nonlinear Optics at Low Intensities using Photon Exchange Interactions", invited paper presented at the Laser Physics '99 Conference, Budapest, Hungary, 3 July, 1999.

J. D. Franson and T. B. Pittman, "Two-Photon Interactions for use in Quantum Computing", invited paper presented at the Quantum Communication, Measurement, and Computing conference, Northwestern University, August 22-27, 1998.

J. D. Franson and T. B. Pittman, "Two-photon nonlinear interactions for use in quantum logic gates", paper presented at the OSA Annual Meeting, Baltimore, MD, Oct. 8, 1998.

J.D. Franson and T.B. Pittman, "Nonlinear Optics at the Two-Photon Level", in International Quantum Electronics Conference, Vol. 7, 1998 OSA Technical Digest Series (Optical Society of America, Washington, DC, 1998).

VII. Participating scientific personnel

J. D. Franson - principal investigator

T. B. Pittman - post-doctoral fellow, now a permanent staff member

B. C. Jacobs - Ph. D. student

VIII. Inventions

J. D. Franson, patent application submitted for "Optical Method for Quantum Computing", June 1, 1999.

IX. Bibliography

1. J. D. Franson and T. B. Pittman, Phys. Rev. A **60**, 917 (1999).
2. R. H. Dicke, Phys. Rev. **93**, 99 (1954).
3. J. D. Franson, Phys. Rev. Lett. **78**, 3852 (1997).
4. G. J. Milburn, Phys. Rev. Lett. **62**, 2124 (1989).
5. Q. A. Turchette, C. J. Hood, W. Lange, H. Mabuchi, and J. H. Kimble, Phys. Rev. Lett. **75**, 4710 (1995).
6. S. E. Harris and Y. Yamamoto, Phys. Rev. Lett. **81**, 3611 (1998).
7. H. Schmidt and A. Imamoglu, Opt. Lett. **21**, 1936 (1996); A. Imamoglu, H. Schmidt, G. Woods, and M. Deutsch, Phys. Rev. Lett. **79**, 1467 (1997); M. M. Kash, V. A. Sautenkov, A. S. Zibrov, L. Hollberg, G. R. Welch, M. D. Lukin, Y. Rostovtsev, E. S. Fry, and M. O. Scully, Phys. Rev. Lett. 82, 5229 (1999).
8. N. Bloembergen, *Nonlinear Optics*, 4th edition (World Scientific, Singapore, 1996).
9. N. A. Kurnit, I. D. Abella, and S. R. Hartmann, Phys. Rev. Lett. **13**, 567 (1964); I. D. Abella, N. A. Kurnit, and S. R. Hartmann, Phys. Rev. **141**, 391 (1966).
10. P. R. Hemmer, and M. S. Shahriar, Phys. Rev. A **59**, R2583 (1999).
11. B. E. A. Saleh and M. C. Teich, Fundamentals of Photonics (Wiley, N.Y., 1991).
12. P. Shor, Phys. Rev. A **52**, 2493 (1995); A. M. Steane, Phys. Rev. Lett. **77**, 793 (1996).
13. C. P. Williams and S. H. Clearwater, *Explorations in Quantum Computing* (Springer-Verlag, N.Y., 1998).
14. P. C. Hemmer, proceedings of the TAMU-ONR Workshop on Quantum Optics, Jackson, Wyoming, July 26-30, 1999 (to be published); R. l. Cone, ibid.; Z. Hasan, ibid.
15. J. D. Franson, Quantum Computing Program Review, Adelphi, MD, Aug. 30-Sept. 2, 1999 (unpublished); Workshop on Fundamental Issues in Quantum Information, Rochester, NY, Oct. 29-31, 1999 (unpublished).
16. R. Krishna Mohan, B. Luo, S. Kroll, and A. Mair, Phys. Rev. A **58**, 4348 (1998); E. Polzik, Workshop on Fundamental Issues in Quantum Information, Rochester, NY, Oct. 29-31, 1999 (unpublished).